Motion and Flow

A Scalar Function Formulation for Optical Flow

Amir A. Amini

Departments of Diagnostic Radiology and Electrical Engineering
Yale University
New Haven, CT 06510

Abstract. In this work, we present results from a new formulation for determining image velocities from a time-sequence of X-ray projection images of flowing fluid. Starting with the conservation of mass principle, and physics of X-ray projection, we derive a motion constraint equation for projection imaging, a practical special case of which is shown to be the Horn and Schunck's optical flow constraint. We are interested in the study of non-rigid motion of blood which is an incompressible fluid, and as such have developed a formulation for optical flow which is applicable to such media. The formulation is particularly efficient, as the flow field is obtained from a 90 degrees rotation applied to the gradient of a scalar function. It is shown that if specific criteria are met, in addition to normal flow which is commonly recoverable, the tangential component of the flow field is also recoverable, bypassing the aperture problem. An algorithm is presented to illustrate this. Preliminary results from the optical flow formulation applied to synthetic images, as well as contrast-injected X-ray images of flowing fluid, in a cylindrical fluid phantom are presented.

1 Introduction

In the past, much of the work in image sequence processing has dealt with motion analysis of rigidly moving objects [1]. Non-rigidity however occurs abundantly in motion of both solids and fluids: motion of trees, muscular motion of faces, and non-rigid movement and pumping motion of the left-ventricle (LV) of the heart, as well as blood motion are all non-rigid. To date, however, most of the work in non-rigid motion has dealt with motion analysis of solid objects [10, 7, 3, 4, 12, 15, 14]. In this paper, we discuss a new framework for optical flow, and apply it to non-rigid motion analysis of blood from a sequence of X-ray projection images.[1] In case of fluids, such as the blood, the clear direction to take is to develop methods capable of estimating the velocity field at all points within the fluid body. Previous work on measurement of optical flow from image sequences may be categorized into four subgroups: (1) differential techniques [9, 11, 13], (2) phase-based techniques [6], (3) region-based technique [5, 16], and (4) spatio-temporal energy techniques [8]. The scalar function formulation for optical flow may be categorized as a differential technique.

[1] We are interested in the potential diagnostic utility of our optical flow methods in characterizing velocity field disturbances in vessels due to atherosclerotic disease.

Lecture Notes in Computer Science, Vol. 800
Jan-Olof Eklundh (Ed.)
Computer Vision – ECCV '94

The paper is organized into two parts. In the first part, a general motion constraint equation for X-ray projection imagery is derived. To derive this equation, the conservation of mass principle is applied to flowing blood and the injected contrast medium, which attenuates the X-rays, in order to obtain an equation relating partial derivatives of a sequence of X-ray projection pictures with image velocities. Horn and Schunck's optical flow constraint is found to be a practical special case of this constraint. In the second part, the scalar function formulation for optical flow is presented.

2 Motion Constraint Equation for X-ray Imaging

We start by applying the conservation of mass principle to flowing blood in a non-branching vessel. We will refer to density of blood as ρ_b, and assume that ρ_b is constant, the requirement for an incompressible fluid. Then, in any given region of interest, the rate of change of amount of blood mass must be the same as the amount of flux of blood mass across the boundary of that region, so that we have:

$$\frac{\partial}{\partial t}\int \rho_b dA + \int_{\partial A} (\rho_b \mathbf{v}.\mathbf{n}) ds = 0 \tag{1}$$

where $\mathbf{v}$ is the blood velocity, n is normal to the boundary of the region ∂A, and ds is the differential of length element along the boundary of region. The second integral along ∂A is the blood mass flux. Upon invoking Gauss's theorem, we have the continuity equation involving blood density and blood velocity:

$$\frac{\partial \rho_b}{\partial t} + \nabla \cdot (\rho_b \mathbf{v}) = 0 \tag{2}$$

with ρ_b constant, the above equation simplifies to

$$\nabla \cdot \mathbf{v} = 0 \tag{3}$$

which is the condition for incompressibility of blood, the divergence-free constraint. In X-ray imaging, blood will not be visible in itself, and a contrast material must be injected in to the blood stream, resulting in attenuation of the X-rays. The contrast velocity will obey blood velocity, $\mathbf{v}$,

$$\frac{\partial \rho_c}{\partial t} + \nabla \cdot (\rho_c \mathbf{v}) = 0 \tag{4}$$

Since the divergence of blood velocity must be zero, the above equation reduces to

$$\frac{\partial \rho_c}{\partial t} + \mathbf{v} \cdot \nabla \rho_c = 0 \tag{5}$$

Assuming monochromatic X-ray beams, for X-ray projection imaging,

$$\log \frac{E}{E_0} = -\left\{ BL(l) + \int_0^l \mu_c \rho_c (\beta(u)) ds \right\} \tag{6}$$

where $E = E(\beta(l))$ is the image intensity that results when one follows the actual path of an X-ray beam up to the point $\beta(l) = (x(l), y(l), z(l))$, u parametrizes the X-ray beam path through the vessel, E_0 denotes the unattenuated X-rays, μ_c is the mass attenuation coefficient of contrast material and $L(l)$ is the length of path traversed by the beam. B is used to denote the combined attenuation effects in the absence of contrast material. Given this relationship, one can obtain the actual contrast material density at a point, assuming the X-ray beam travel a straight path from a source point, (x_s, y_s, z_s):

$$\rho_c(x, y, z) = \frac{1}{\mu_c} \left\{ \frac{-\nabla E}{E} \right\} \cdot \hat{r}(x, y, z) - \frac{B}{\mu_c} \tag{7}$$

where $\hat{r}(x, y, z)$ is a unit vector pointing from the source towards a point with coordinates (x, y, z). The above equation may be substituted back into (5) to result in a general equation in terms of E, and the components of the vector in the direction of the X-ray beam emanating from the source at (x_s, y_s, z_s). If the source can be assumed to emanate parallel beams, $\rho_c(x, y, z) = -\frac{1}{\mu_c}\{B + \frac{E_z}{E}\}$, resulting in the following equation of continuity for the intensity in terms of blood velocities:

$$\begin{aligned} &E_z E_t - E E_{zt} + (E_x E_z - E E_{xz})u + \\ &(E_y E_z - E E_{yz})v + (E_z^2 - E E_{zz})w = 0 \end{aligned} \tag{8}$$

where partial derivatives are taken with respect to x, y, z, t; all subscripted accordingly. In addition, u,v, and w are each functions representing the x, y, and z components of $\mathbf{v}$ at a point.

With a 2D flow approximation of 3D blood flow, $w = 0$. Furthermore, if we assume that on the average, the distribution of contrast mass can be described by a 2D function, $\rho_c(x, y, z) = \rho_c(x, y)$. The following equation is then obtained as a special case of equation (8):

$$E_t + uE_x + vE_y = 0 \tag{9}$$

describing the components of blood velocities in terms of partial derivatives of contrast-injected pictures. Note that the above equation is the well-known Horn and Schunck's optical flow constraint and relates the partial derivatives of a sequence of images at a point, with the velocity of points on a moving object [9]. Here, we have shown a general form of this equation for X-ray images starting from the conservation of mass principle, and derived (9) as a practical special case for our application. In passing, we note that the natural extension of (9) to 3-space may be directly applied to 3D imaging methods.

3 Scalar Function Formulation

The formulation is based on computing a scalar function that approximately enforces a constraint of the form given in equation (9) for the velocity field, and at the same time the divergence-free condition is readily and exactly satisfied.

In 2D, one can always define a scalar function Ψ such that the velocity field is expressed as

$$\mathbf{v} = \hat{z} \times \nabla\Psi \tag{10}$$

where $\hat{z}$ is a unit vector perpendicular to the image plane. It can easily be checked that this vector field satisfies the divergence-free property. We will refer to such a function as a stream function. In 3D, a similar function may be defined for axi-symmetric motion.

Note that in the dual problem one determines a curl-free velocity field. Parallel to the definition of stream function Ψ, which provides divergence-free velocity fields, we can define a velocity potential Φ, with

$$\mathbf{v} = \nabla\Phi \tag{11}$$

The curl of $\mathbf{v}$, $\nabla \times \nabla\Phi = 0$. This formulation will be suitable for study of irrotational flow fields.

Substitution of components of (10) into equation (9) results in the following hyperbolic PDE:

$$\Psi_x E_y - \Psi_y E_x + E_t = 0 \tag{12}$$

which is a first order equation whose characteristics [2] are the level curves of the projection pictures, E.

We can perform the following integration along a curve C in order to invert equation (12):

$$\Psi(x, y) = \Psi_0 + \int_{(x_0, y_0)}^{(x,y)} \nabla\Psi \cdot \mathbf{t} ds \tag{13}$$

where Ψ_0 is the value of Ψ at (x_0, y_0) and $\mathbf{t}$ is the tangent to C. If C is a level curve of E, the above integral provides an algorithm for determining the mass flux:

$$\Psi(x, y) = \Psi_0 + \int_{(x_0, y_0)}^{(x,y)} \frac{-E_t}{|\nabla E|} ds \tag{14}$$

Along level curves which wrap around, the integral sum in (14) must vanish.[2] As this is very much data dependent, in general such curves will give rise to singularities in the numerical solution.

[2] Note that the integrand is nothing but the familiar normal flow.

3.1 Regularized Solution

Since it is difficult to predict the behavior of the level curves, a more stable numerical algorithm will involve a least-squares solution with an associated variational principle for finding the stream function Ψ:

$$J[\Psi] = \int\int (\Psi_x E_y - \Psi_y E_x + E_t)^2 + \lambda(\Psi_{xx}^2 + 2\Psi_{xy}^2 + \Psi_{yy}^2)dxdy \quad (15)$$

so that J is minimized. The parameter λ controls the degree of smoothing, and in general is a non-negative function of x and y. Discretizing the above integral on the pixel grid, we obtain a sum with central difference approximations for partial derivatives of Ψ, as well as partial derivatives of $E(x, y)$. Solution of the minimization problem at each pixel is obtained by SOR [2]. As Ψ can only be determined up to an additive constant, we set $\Psi = 0$ on the lower boundary and $\Psi = \Gamma$ on the upper boundary. The latter quantity is the total mass flux in a given vessel with no branchings and may be determined using (14), or with a second variational principle involving Γ.

3.2 Experimental Results

We have performed simulations to validate the promise of the technique in computing velocity fields from X-ray angiograms.

The following 2D simulation involved generating a sequence of images where all the models were identically satisfied. For generating synthetic data, we assumed, $\Psi(x, y) = \frac{y}{Y}\Gamma$, with $y \in [0, Y]$ so that $\mathbf{v} = (-\frac{\Gamma}{Y}, 0)$. This would be the case for example, for inviscid flow. We also assumed, $E(x, y) = -\frac{E_0}{X} \cdot x(x - X)$, with $x \in [0, X]$ so that $E_t = -\mathbf{v} \cdot \nabla E = \frac{-2\Gamma E_0}{XY}x + \frac{E_0\Gamma}{Y}$. Using central difference approximation, we then have, $E(x, y, t + \Delta t) = 2\Delta t E_t + E(x, y, t - \Delta t)$. With E_t as given, we generated the first few frames in the sequence with $\Gamma = 128$, $E_0 = 4$, and $X = Y = 128$. Note that in this case at $x = \frac{X}{2}$ the image gradient vanishes. The results are shown in figure 1.

We have just begun with our *in vitro* phantom experiments. The experimental model is a latex tube with an inner diameter of 1.27 cm. X-ray angiography is performed on a GE Advantx digital imaging system at the 6" image intensifier field, with 1024 × 1024 acquisitions at rapid frame rates. For the experiment shown in figure 2, a pump delivered 612 ml/min of water continuously, and 5 ml/sec of an iodine contrast agent was injected for 2 seconds. In order to assess the overall effectiveness of the methodology, soon we will be carrying out statistical testing of the velocity field measurements against known velocities and volumetric flow rates. Further *in vitro* validations of methods and integration with MR-based flow estimation techniques are also planned.

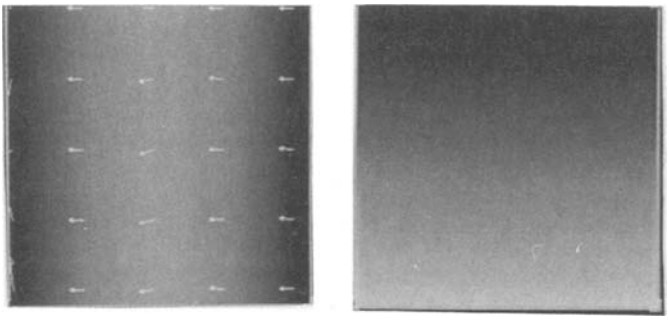

Fig. 1. Left: Sampled velocity field overlaid on the second picture of a simulated sequence for left translating flow. Right: The computed stream function.

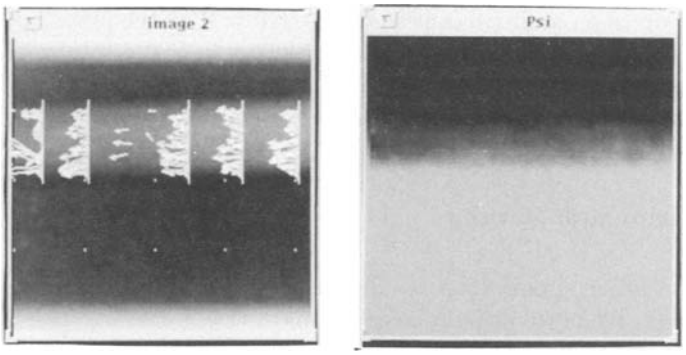

Fig. 2. Left: cross-sectional velocity profiles computed from 3 frames in a phantom sequence, overlaid on the middle frame. Note that the picture is displayed in *reverse video*. Right: The computed stream function from image frames.

4 Conclusions

In conclusions, we have presented results from a new formulation for optical flow. The formulation is computationally efficient, as one needs to compute a single scalar function. As a byproduct, the incompressibility condition on the resulting vector field is automatically satisfied. In the dual problem, the vorticity of the resulting vector field will automatically be zero. We also derived a general motion constraint equation for X-ray imaging starting from the conservation of mass principle and X-ray physics, and derived the Horn and Schunck's optical flow constraint as a practical special case. In the numerical solution, we discussed sources for instabilities, and linked such behavior with wrap around of level curves of E. In fact, along well-behaved level curves, the normal flow can

be integrated to yield the full flow field. Note that this statement has deeper implications: that is, in addition to the normal component of the velocity field, in the absence of bad characteristics, the tangential component is recoverable, bypassing the aperture problem.

References

1. J. K. Aggarwal. Motion and time-varying imagery – an overview. In *Proceedings of the Workshop on Visual Motion*, 1986.
2. William F. Ames. *Numerical Methods for Partial Differential Equations*. Academic Press, New York, 1992.
3. A. A. Amini, R. W. Curwen, R. T. Constable, and J. C. Gore. Mr physics-based snake tracking and dense deformations from tagged cardiac images. In *AAAI Symposium on Applications of Computer Vision to Medical Image Processing*, Stanford University, Stanford, California, March 21-23 1994.
4. A. A. Amini and J. S. Duncan. Bending and stretching models for lv wall motion analysis from curves and surfaces. *Image and Vision Computing*, 10(6):418–430, July/August 1992.
5. P. Anandan. A computational framework and an algorithm for the measurement of visual motion. *International Journal of Computer Vision*, 2:283–310, 1989.
6. D. Fleet and A. Jepson. Computation of component image velocity from local phase information. *International Journal of Computer Vision*, 5:77–104, 1990.
7. D. Goldgof, H. Lee, and T. Huang. Motion analysis of nonrigid surfaces. In *Proceedings of IEEE conference on Computer Vision and Pattern Recognition*, 1988.
8. D. Heeger. Optic flow using spatio-temporal filters. *International Journal of Computer Vision*, 1:279–302, 1988.
9. B.K.P. Horn and B. G. Schunck. Determining optical flow. *Artifical Intelligence*, 1981.
10. T. Huang. Modeling, analysis, and visualization of nonrigid object motion. In *International Conference on Pattern Recognition*, 1990.
11. B. Lucas and T. Kanade. An iterative image registration technique with an application to stereo vision. In *Proc. DARPA IU Workshop*, pages 121–130, 1981.
12. D. Metaxas and D. Terzopoulos. Recursive estimation of shape and nonrigid motion. In *IEEE Workshop on Visual Motion*, pages 306–311, 1991.
13. H. H. Nagel. On the estimation of optic flow: Relations between different approaches and some new results. *Artificial Intelligence*, 33:299–324, 1987.
14. C. Nastar and N. Ayache. Non-rigid motion analysis in medical images: A physically based approach. In *Information Processing in Medical Imaging*, pages 17–32, 1993.
15. A. Pentland, B. Horowitz, and S. Sclaroff. Non-rigid motion and structure from contour. In *IEEE Workshop on Visual Motion*, pages 288–293, 1991.
16. A. Singh. An estimation theoretic framework for image-flow computation. In *Proc. International Conference on Computer Vision*, pages 168–177, Osaka, Japan, 1990.